International Conference on Control, Engineering & Information Technology (CEIT'14)

Proceedings - Copyright IPCO-2014, pp.340-344

ISSN 2356-5608

High performance PISM of photovoltaic system

Asma CHIHI
Research Unit C3S
ESSTT
Tunis, Tunisia
asma.chihi@live.fr

Adel CHBEB
Research Unit C3S
ESSTT
Tunis, Tunisia
adel.chbeb@enib.rnu.tn

Anis SELLAMI
Research Unit C3S
ESSTT
Tunis, Tunisia
Anis.Sellami@esstt.rnu.tn

Abstract—**This paper presents a new technique for indirect field oriented control by sliding mode applied to a photovoltaic system. The proposed method is based on adding an integral action to the switching function defining the control strategy. A comparative study was conducted to test the performance of this control. Finally, a simulation results is presented to show the effectiveness of this method.**

Keywords-component; Photovoltaic, Induction Motor (IM), Indirect Field Oriented Control (IFOC), Proportional Integral Sliding Mode (PISM).

I. INTRODUCTION

The unavailability of electricity in isolated sites such as oil and irrigation, also the very high cost of energy distribution led to the use of renewable sources like photovoltaic energy, which is considered, today, as an important element of electrical energy totally clean.

This latter admits several benefits that are responsible for its development and its implementation in various areas of applications. Since it is inexhaustible, characterized by high reliability, requires less maintenance and adapts the needs of each project. This type of energy is generally suited to electrical machines such as induction motor, which his model is strongly nonlinear. This is clearly from the differential equations modeling the machine. View its area of application and its use in extremely aggressive conditions like: the oil application, maritime and rail traction, etc [1]. The machine submitted to internal parametric variations namely: variation of the stator or rotor resistances, leakage inductance, etc. Those are caused to external disturbances such as temperature variation, load variation and variation of the isolation value of the machine, etc. These unexpected disturbances require to an adaptive control law that can compensate for these variations and maintain the robustness of the system.

The sliding mode control is one of the techniques who satisfy the requirements of this problem [2], [3], [5] and [7]. In this paper, we interested to design a field oriented control by sliding mode [9] and [10]. The main purpose is the choice comes at the sliding surface which an integral term is added.

This paper is organized into seven sections. After the introduction, the problem statement is presented. The third section describes the dynamic system. Then, the control law design is proposed. In section five the simulation results are interpreted and discussed to validate the best control method. Then, a comparative study is determined. Finally, a conclusion is drawn.

II. PROBLEM STATEMENT

The main problem of this paper divides into two parts:

On the one hand, photovoltaic energy depends on natural parameters such as sunshine and ambient temperature. The two latter are variable and uncontrollable by humans. This makes the power available at the panel random varies. So, we will need to find the maximum power available at the panel and also have a control able to maintain the maximum power in term optimum energy transfer required by the load.

In the other hand, many applications using the induction motor requires a torque and speed accuracy, also robustness against the parametric variations. For this reason, we must find a control that can satisfy the performances introduced to the system.

III. SYSTEM PRESENTATION

The proposed system is constituted by an induction motor supplied by a photovoltaic source through a converter DC/DC and an inverter. The purpose is to achieve a field oriented control by sliding mode; the principle is summarized to the choice of the sliding surface that is carried with different methods namely: proportional and proportional integral controllers.

The general proposed scheme is as follows:

International Conference on Control, Engineering & Information Technology (CEIT'14)

Proceedings - Copyright IPCO-2014, pp.340-344

ISSN 2356-5608

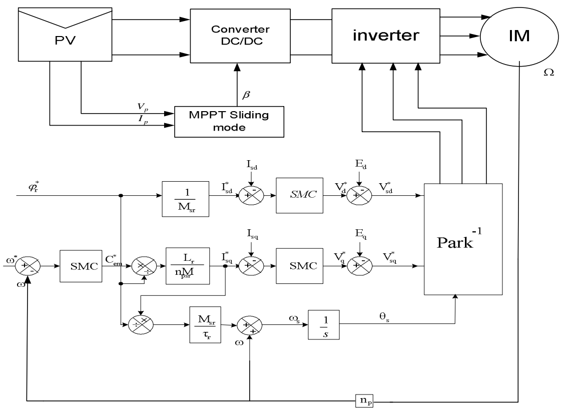

Figure 1. Structure of photovoltaic system

The mathematical model of the induction motor is defined by:

$$\begin{cases} \dfrac{di_{sd}}{dt} = -(\dfrac{1}{\sigma\tau_s} + \dfrac{1-\sigma}{\sigma\tau_r}) i_{sd} + \dfrac{1-\sigma}{\sigma M_{sr}\tau_r}\varphi_{rd} + \dfrac{1-\sigma}{\sigma M_{sr}}\varphi_{rq}\, w + \dfrac{1}{\sigma L_s} V_{sd} \\ \dfrac{di_{sq}}{dt} = -w_{dq}\, i_{sd} - (\dfrac{1}{\sigma\tau_s} + \dfrac{1-\sigma}{\sigma\tau_r}) i_{sq} - \dfrac{1-\sigma}{\sigma M_{sr}} w\,\varphi_{rd} + \dfrac{1-\sigma}{\sigma M_{sr}\tau_r}\varphi_{rq} + \dfrac{1}{\sigma L_s} V_{sq} \\ \dfrac{d\varphi_{rd}}{dt} = \dfrac{M_{sr}}{\tau_r} i_{sd} - \dfrac{1}{\tau_r}\varphi_{rd} - w\,\varphi_{rq} \\ \dfrac{d\varphi_{rq}}{dt} = \dfrac{M_{sr}}{\tau_r} i_{qs} + w\,\varphi_{dr} - \dfrac{1}{\tau_r}\varphi_{qr} \\ \dfrac{dw}{dt} = \dfrac{3}{2}\dfrac{np^2}{j}\dfrac{M_{sr}}{L_r}(\varphi_{rd}\, i_{sq} - \varphi_{rq}\, i_{sd}) - \dfrac{np}{j}(C_r - C_f) \end{cases} \quad (1)$$

With

i_{ds}, i_{qs} : d-, q-axis stator current components,

$\varphi_{dr}, \varphi_{qr}$: d-, q-axis rotor flux components,

w_{sl} : slip angular speed (w_{dq}-w_r),

w_{dq} : synchronious angular speed,

R_r, R_s : rotor and stator resistances,

M_{sr} : cyclic mutual inductance stator-rotor,

L_r, L_s : rotor and stator self-inductions,

τ_s, τ_r : stator and rotor time constant,

σ : leakage coefficient,

np : pole-pair number,

j : inertia,

C_f : friction torque,

C_r : load torque,

t : Continuous time.

IV. SLIDING MODE CONTROL (SMC)

The concept of sliding mode control can be summarized in three steps: choice of sliding surface, reaching conditions and determination of control law [4], [8], [11] and [12].

A. *Sliding surface design*

Generally, several researchers have used the sliding surfaces which are defined as [1], [13] and [14]:

$$\begin{cases} s_v = c_1\varepsilon_v & with\ \ \varepsilon_v = V_p^* - V_p \\ s_w = c_2\varepsilon_w & with\ \ \varepsilon_w = w^* - w \\ s_d = c_3\varepsilon_d & with\ \ \varepsilon_d = I_{sd}^* - I_{sd} \\ s_q = c_4\varepsilon_q & with\ \ \varepsilon_q = I_{sq}^* - I_{sq} \end{cases} \quad (2)$$

However, due the complexity of the real system, we ameliorate the dynamic of the switching function, that we added an integral term in order to obtain a faster response time and zero steady-state error. The new proposed sliding surfaces are presented as follows:

$$\begin{cases} s_v = c_1\varepsilon_v + c_5\int \varepsilon_v dt \\ s_w = c_2\varepsilon_w + c_6\int \varepsilon_w dt \\ s_d = c_3\varepsilon_d + c_7\int \varepsilon_d dt \\ s_q = c_4\varepsilon_q + c_8\int \varepsilon_q dt \end{cases} \quad (3)$$

Where:

$c_1, c_2, c_3, c_4, c_5, c_6, c_7, c_8$: proportional gains.

B. *Determination of control law*

The control law design of the photovoltaic system is constituted by four control loops relative to the four selected switching functions.

- *MPPT control*

The switching function is presented by:

$$s_v = c_1\varepsilon_v + c_5\int \varepsilon_v dt \quad (4)$$

The fundamental equation relative to the photovoltaic is as follows:

$$\dot{V}_p = \frac{I_{ph}}{C_p} - \frac{I_{ss}}{C_p}(e^{\frac{V_p}{V_t}} - 1) + \frac{1}{C_p(1-\beta)} I_s \quad (5)$$

With

International Conference on Control, Engineering & Information Technology (CEIT'14)

Proceedings - Copyright IPCO-2014, pp.340-344

ISSN 2356-5608

V_p : output voltage of the PV cell
I_{ph} : photo current of the PV cell,
I_{ss} : saturation current of the diode,
V_t : thermodynamic potential of PV cell
β : duty cycle

The control law is determined by:

$$V_p^* = \frac{1}{I_s}(I_{ph} - I_{ss}(e^{\frac{V_p}{V_t}} - 1)) - k_v |s_v|^\alpha sign(s_v) \quad with \;\; 0 < \alpha < 1 \tag{6}$$

- *Speed controller*

The representative switching functions is expressed as follows:

$$s_\omega = c_2\varepsilon_\omega + c_6\int \varepsilon_\omega dt \tag{7}$$

The time derivative of Eqn. (7) is given as:

$$\dot{s}_\omega = c_2\dot{\varepsilon}_\omega + c_6\varepsilon_\omega \tag{8}$$

The mechanical equation is defined by:

$$j\frac{dw}{dt} + f_r w = np(C_{em} - C_r) \tag{9}$$

Where the control law is C_{em}^* :

$$C_{em}^* = C_{em\_eq} + C_{em\_nl} \tag{10}$$

During the sliding mode, we have: $s_w = \dot{s}_w = 0$.

The global control functions as follows:

$$C_{em}^* = \frac{J}{np}(\dot{w}^* + \frac{f}{J}w + \frac{c_6}{c_2}\varepsilon_w) - k_w|s_w|^\alpha sign(s_w) \quad with \;\; 0<\alpha<1 \tag{11}$$

Where:

k_w: Proportional gain of the nonlinear control relative to the speed controller,

$sign(.)$: Signum function.

- *Direct stator current controller*

The switching function relative to the direct stator current controller is defined as:

$$s_d = c_3\varepsilon_d + c_7\int \varepsilon_d dt \tag{12}$$

The time derivative of the switching function in Eqn. (12) is:

$$\dot{s}_d = c_3\dot{\varepsilon}_d + c_7\varepsilon_d \tag{13}$$

The control law V_d^* is given by:

$$V_d^* = V_{d\_eq} + V_{d\_nl} \tag{14}$$

From Eqns. (12)–(14), we get:

$$V_d^* = \sigma L_s(\dot{I}_{sd}^* + (\frac{1}{\sigma\tau_s} + \frac{(1-\sigma)}{\sigma\tau_r})i_{sd} + \frac{c_7}{c_3}\varepsilon_d) - k_d|s_d|^\alpha sign(s_d) \tag{15}$$

$with \;\; 0<\alpha<1$

Where:

k_d : Proportional gain of the nonlinear control relative to the speed controller.

- *Quadratic stator current controller*

The representative equation defining the switching function relative to the quadratic stator current is given by:

$$s_q = c_4\varepsilon_q + c_8\int \varepsilon_q dt \tag{16}$$

We consider the time derivative of Eqn. (16) is donated as:

$$\dot{s}_q = c_4\dot{\varepsilon}_q + c_8\varepsilon_q \tag{17}$$

The control law V_q^* is presents by:

$$V_q^* = V_{q\_eq} + V_{q\_nl} \tag{18}$$

During the sliding mode: $s_q = \dot{s}_q = 0$.

The global control law is summarized as follows:

$$V_q^* = \sigma L_s(\dot{I}_{sq}^* + (\frac{1}{\sigma\tau_s} + \frac{(1-\sigma)}{\sigma\tau_r})i_{sq} + \frac{c_8}{c_4}\varepsilon_d) - k_q|s_q|^\alpha sign(s_q) \tag{19}$$

$with \;\; 0<\alpha<1$

Where:

k_q: Proportional gain of the nonlinear control relative to the speed controller.

C. Reaching conditions

The existence condition of sliding mode advert that both s and $\dot{s}$ will tends to zero when t tend to infinity, Let us consider the Lyapunov function candidate:

$$V = \frac{1}{2}s^2 \tag{20}$$

The condition leads to the following inequality:

$$s.\dot{s} < 0 \tag{21}$$

We applied the condition given by Eqn. (21), we can note that:

$$k_v > 0 \;\; k_w > \frac{j}{c_1 \; np}, \; k_d > \frac{\sigma L_s}{c_2} \text{ and } k_q > \frac{\sigma L_s}{c_3}.$$

V. Results and Discussion

In this section, we are going to examine the performance of the proposed control developed above. In the first step, we visualized the switching functions that are converged to zero. This is satisfying the criteria of sliding mode, Figure 2.

International Conference on Control, Engineering & Information Technology (CEIT'14)

Proceedings - Copyright IPCO-2014, pp.340-344

ISSN 2356-5608

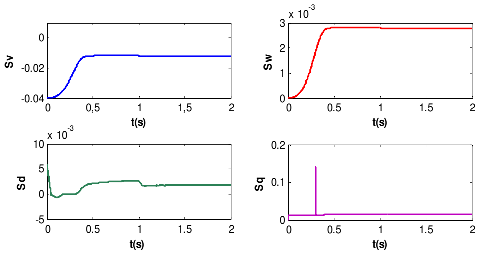

Figure 2. Evolution of the sliding surfaces

The second step, we are supposed to show the evolution of the torque. Initially, it starts without load. Then, we insert a load torque value 2Nm from instant 1s, Fig. 3.

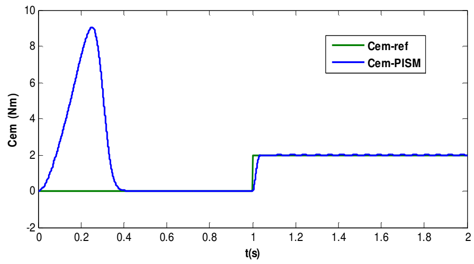

Figure 3. Evolution of the torque

VI. Comparative Study

Sometimes, the systems required robustness and other systems precision. The dilemma between robustness and precision is still a research topic. The proposed control combines the advantages of both.

A. *Precision*

In this section, a comparative study between different regulators, such as: conventional PI, PSM and PISM, is presented for testing the precision of the system.

In this context, it is necessary to calculate the error applied to the torque. We can conclude that the respective error with PSM is most elevated than the conventional PI and PISM, Figure 4.

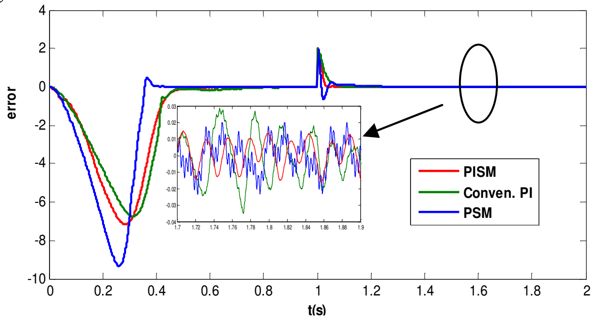

Figure 4. Representative error of the torque with different methods

Table 1 resume the steady state error and settling time measured from conventional PI, PSM and PISM. The best results are provided with PISM, we interpreted that the adding of the integral action given to the switching function ameliorates the precision of the system.

TABLE I. Comparison results for precision test with different techniques

	Conventional PI	***PSM***	***PISM***
Steady state error	0.020	0.025	0.010
Settling time	0.450	0.350	0.210

B. *Robustness*

Like any kind of control, it is necessary to testing the robustness for this latter by applying uncertainties for parameter of the system. For this, we will vary the rotor inductance L_r to -20% its nominal value.

Figure 5 presents the rotor inductance variation; we concluded that the response with conventional PI is changed. Moreover, with sliding mode has not changed. This verified the robustness provided to the proposed control

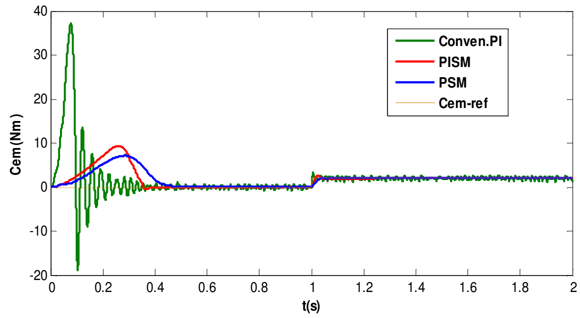

Figure 5. Robustness test with -20% of rotor inductance variation

VII. Conclusion

In this paper, a new indirect field oriented control applied to a photovoltaic system is presented. The proposed technique is obtained from choice of the switching function. It is clear that the performance given by the adding of the integral action provides the best results.

Appendix

Induction motor parameters:

- 85/140V
- 3.5/6A
- f =50Hz
- $R_s = 3.45\Omega$

Proceedings - Copyright IPCO-2014, pp.340-344

ISSN 2356-5608

- $R_r = 2.95\Omega$
- $L_s = 0.1442\text{H}$
- $L_r = 0.1442\text{H}$
- $M_{sr} = 0.1342\text{H}$
- $j = 0.01\text{Kgm2}$
- $np = 2$

REFERENCES

[1] A. Chihi, A. Sallami and A. Kalfa, Sliding mode control of a photovoltaic pumping system, , IEEE-MELECON-2012.pp: 936-939.

[2] M. A. Fnaiech, F. Betin, F. Fnaiech, G. A. Capolino, Sliding Mode Control for Dual Three-phase Induction Motor Drives, IEEE ISIE, Montreal, Quebec, Canada, July 2006, pp. 9-12.

[3] A. H. Obeid Ahmed, M. O. Ajangnay, S. A. Mohamed, Ma. W. Dunnigan, Speed Control of Induction Motor Using New Sliding Mode Control Technique, 1st International Conference on Energy, Power and Control (EPC-IQ), College of Engineering, University of Basrah, 2010.

[4] V. I. Utkin, Sliding mode control design principles and applications to electric drives, IEEE transactions industrial electronics, Vol. 40, No. 1, February 1993, pp. 23-36.

[5] D. Dal, Sensorless Sliding Mode Direct Torque Control (DTC) of Induction Motor, IEEE ISIE 2005, June 2005, pp. 20-23.

[6] A. Sabanovic and D.B.Izosimov, Application of sliding modes to induction motor control, IEEE transactions on industry applications, Vol. 1A-17, 1981, pp.41-49.

[7] W. Gao and J. C. Hung, Variable structure control for nonlinear systems: A new approach, IEEE transactions on industrial electronics, Vol. 40, February 1993, pp. 2–22.

[8] M. Moallem, B. Mirzaeian, O. A. Mohammed, and C. Lucas, Multi-Objective Genetic-Fuzzy Optimal Design of PI Controller in the Indirect Field Oriented Control of an Induction Motor, IEEE Transactions On magnetics, Vol. 37, No. 5, September 2001, pp. 3608–3612.

[9] D. Lee, S. Sul, and M. Park, High Performance Current Regulator for a Field-Oriented Controlled Induction Motor Drive, IEEE Transactions on industry applications, Vol. 30, No. 5, September/October 1994, pp. 1247-1257.

[10] S. Rao, M. Buss and V. Utkin, Sliding Mode based Stator Flux and Speed Observer for Induction Machines, IEEE international journal of variable structure systems, 2008, pp-95-99.

[11] A. Sabanovic, Variable Structure Systems with Sliding Modes in Motion Control- A Survey, IEEE Transaction Ind. Inf., vol 7, No.2, May 2011, pp. 212–223.

[12] M. Ellouze, R. Gamoudi1 and A. Mami, Sliding mode control applied to a photovoltaic water pumping system, International Journal of Physical Sciences, Vol. 5(4), April 2010, pp. 334-344.

[13] A. Msaddek, A. Gaaloul, and F.M'sahli, A Novel Higher Order Sliding Mode Control: Application to an Induction Motor, International conference on Control, Engineering & information technology (CEIT'13).